arXiv:0808.0900 [hep-ex]
SLAC-PUB-13356
BABAR-PUB-08/033

Search for the highly suppressed decays $B^- \to K^+\pi^-\pi^-$ and $B^- \to K^-K^-\pi^+$

B. Aubert,[1] M. Bona,[1] Y. Karyotakis,[1] J. P. Lees,[1] V. Poireau,[1] E. Prencipe,[1] X. Prudent,[1] V. Tisserand,[1] J. Garra Tico,[2] E. Grauges,[2] L. Lopez[ab],[3] A. Palano[ab],[3] M. Pappagallo[ab],[3] G. Eigen,[4] B. Stugu,[4] L. Sun,[4] G. S. Abrams,[5] M. Battaglia,[5] D. N. Brown,[5] R. N. Cahn,[5] R. G. Jacobsen,[5] L. T. Kerth,[5] Yu. G. Kolomensky,[5] G. Lynch,[5] I. L. Osipenkov,[5] M. T. Ronan,[5,*] K. Tackmann,[5] T. Tanabe,[5] C. M. Hawkes,[6] N. Soni,[6] A. T. Watson,[6] H. Koch,[7] T. Schroeder,[7] D. Walker,[8] D. J. Asgeirsson,[9] B. G. Fulsom,[9] C. Hearty,[9] T. S. Mattison,[9] J. A. McKenna,[9] M. Barrett,[10] A. Khan,[10] V. E. Blinov,[11] A. D. Bukin,[11] A. R. Buzykaev,[11] V. P. Druzhinin,[11] V. B. Golubev,[11] A. P. Onuchin,[11] S. I. Serednyakov,[11] Yu. I. Skovpen,[11] E. P. Solodov,[11] K. Yu. Todyshev,[11] M. Bondioli,[12] S. Curry,[12] I. Eschrich,[12] D. Kirkby,[12] A. J. Lankford,[12] P. Lund,[12] M. Mandelkern,[12] E. C. Martin,[12] D. P. Stoker,[12] S. Abachi,[13] C. Buchanan,[13] J. W. Gary,[14] F. Liu,[14] O. Long,[14] B. C. Shen,[14,*] G. M. Vitug,[14] Z. Yasin,[14] L. Zhang,[14] V. Sharma,[15] C. Campagnari,[16] T. M. Hong,[16] D. Kovalskyi,[16] M. A. Mazur,[16] J. D. Richman,[16] T. W. Beck,[17] A. M. Eisner,[17] C. J. Flacco,[17] C. A. Heusch,[17] J. Kroseberg,[17] W. S. Lockman,[17] A. J. Martinez,[17] T. Schalk,[17] B. A. Schumm,[17] A. Seiden,[17] M. G. Wilson,[17] L. O. Winstrom,[17] C. H. Cheng,[18] D. A. Doll,[18] B. Echenard,[18] F. Fang,[18] D. G. Hitlin,[18] I. Narsky,[18] T. Piatenko,[18] F. C. Porter,[18] R. Andreassen,[19] G. Mancinelli,[19] B. T. Meadows,[19] K. Mishra,[19] M. D. Sokoloff,[19] P. C. Bloom,[20] W. T. Ford,[20] A. Gaz,[20] J. F. Hirschauer,[20] M. Nagel,[20] U. Nauenberg,[20] J. G. Smith,[20] K. A. Ulmer,[20] S. R. Wagner,[20] R. Ayad,[21,†] A. Soffer,[21,‡] W. H. Toki,[21] R. J. Wilson,[21] D. D. Altenburg,[22] E. Feltresi,[22] A. Hauke,[22] H. Jasper,[22] M. Karbach,[22] J. Merkel,[22] A. Petzold,[22] B. Spaan,[22] K. Wacker,[22] M. J. Kobel,[23] W. F. Mader,[23] R. Nogowski,[23] K. R. Schubert,[23] R. Schwierz,[23] A. Volk,[23] D. Bernard,[24] G. R. Bonneaud,[24] E. Latour,[24] M. Verderi,[24] P. J. Clark,[25] S. Playfer,[25] J. E. Watson,[25] M. Andreotti[ab],[26] D. Bettoni[a],[26] C. Bozzi[a],[26] R. Calabrese[ab],[26] A. Cecchi[ab],[26] G. Cibinetto[ab],[26] P. Franchini[ab],[26] E. Luppi[ab],[26] M. Negrini[ab],[26] A. Petrella[ab],[26] L. Piemontese[a],[26] V. Santoro[ab],[26] R. Baldini-Ferroli,[27] A. Calcaterra,[27] R. de Sangro,[27] G. Finocchiaro,[27] S. Pacetti,[27] P. Patteri,[27] I. M. Peruzzi,[27,§] M. Piccolo,[27] M. Rama,[27] A. Zallo,[27] A. Buzzo[a],[28] R. Contri[ab],[28] M. Lo Vetere[ab],[28] M. M. Macri[a],[28] M. R. Monge[ab],[28] S. Passaggio[a],[28] C. Patrignani[ab],[28] E. Robutti[a],[28] A. Santroni[ab],[28] S. Tosi[ab],[28] K. S. Chaisanguanthum,[29] M. Morii,[29] A. Adametz,[30] J. Marks,[30] S. Schenk,[30] U. Uwer,[30] V. Klose,[31] H. M. Lacker,[31] D. J. Bard,[32] P. D. Dauncey,[32] J. A. Nash,[32] M. Tibbetts,[32] P. K. Behera,[33] X. Chai,[33] M. J. Charles,[33] U. Mallik,[33] J. Cochran,[34] H. B. Crawley,[34] L. Dong,[34] W. T. Meyer,[34] S. Prell,[34] E. I. Rosenberg,[34] A. E. Rubin,[34] Y. Y. Gao,[35] A. V. Gritsan,[35] Z. J. Guo,[35] C. K. Lae,[35] N. Arnaud,[36] J. Béquilleux,[36] A. D'Orazio,[36] M. Davier,[36] J. Firmino da Costa,[36] G. Grosdidier,[36] A. Höcker,[36] V. Lepeltier,[36] F. Le Diberder,[36] A. M. Lutz,[36] S. Pruvot,[36] P. Roudeau,[36] M. H. Schune,[36] J. Serrano,[36] V. Sordini,[36,¶] A. Stocchi,[36] G. Wormser,[36] D. J. Lange,[37] D. M. Wright,[37] I. Bingham,[38] J. P. Burke,[38] C. A. Chavez,[38] J. R. Fry,[38] E. Gabathuler,[38] R. Gamet,[38] D. E. Hutchcroft,[38] D. J. Payne,[38] C. Touramanis,[38] A. J. Bevan,[39] C. K. Clarke,[39] K. A. George,[39] F. Di Lodovico,[39] R. Sacco,[39] M. Sigamani,[39] G. Cowan,[40] H. U. Flaecher,[40] D. A. Hopkins,[40] S. Paramesvaran,[40] F. Salvatore,[40] A. C. Wren,[40] D. N. Brown,[41] C. L. Davis,[41] A. G. Denig,[42] M. Fritsch,[42] W. Gradl,[42] G. Schott,[42] K. E. Alwyn,[43] D. Bailey,[43] R. J. Barlow,[43] Y. M. Chia,[43] C. L. Edgar,[43] G. Jackson,[43] G. D. Lafferty,[43] T. J. West,[43] J. I. Yi,[43] J. Anderson,[44] C. Chen,[44] A. Jawahery,[44] D. A. Roberts,[44] G. Simi,[44] J. M. Tuggle,[44] C. Dallapiccola,[45] X. Li,[45] E. Salvati,[45] S. Saremi,[45] R. Cowan,[46] D. Dujmic,[46] P. H. Fisher,[46] G. Sciolla,[46] M. Spitznagel,[46] F. Taylor,[46] R. K. Yamamoto,[46] M. Zhao,[46] P. M. Patel,[47] S. H. Robertson,[47] A. Lazzaro[ab],[48] V. Lombardo[a],[48] F. Palombo[ab],[48] J. M. Bauer,[49] L. Cremaldi,[49] R. Godang,[49,**] R. Kroeger,[49] D. A. Sanders,[49] D. J. Summers,[49] H. W. Zhao,[49] M. Simard,[50] P. Taras,[50] F. B. Viaud,[50] H. Nicholson,[51] G. De Nardo[ab],[52] L. Lista[a],[52] D. Monorchio[ab],[52] G. Onorato[ab],[52] C. Sciacca[ab],[52] G. Raven,[53] H. L. Snoek,[53] C. P. Jessop,[54] K. J. Knoepfel,[54] J. M. LoSecco,[54] W. F. Wang,[54] G. Benelli,[55] L. A. Corwin,[55] K. Honscheid,[55] H. Kagan,[55] R. Kass,[55] J. P. Morris,[55] A. M. Rahimi,[55] J. J. Regensburger,[55] S. J. Sekula,[55] Q. K. Wong,[55] N. L. Blount,[56] J. Brau,[56] R. Frey,[56] O. Igonkina,[56] J. A. Kolb,[56] M. Lu,[56] R. Rahmat,[56] N. B. Sinev,[56] D. Strom,[56] J. Strube,[56] E. Torrence,[56] G. Castelli[ab],[57] N. Gagliardi[ab],[57] M. Margoni[ab],[57] M. Morandin[a],[57] M. Posocco[a],[57] M. Rotondo[a],[57] F. Simonetto[ab],[57] R. Stroili[ab],[57] C. Voci[ab],[57] P. del Amo Sanchez,[58] E. Ben-Haim,[58] H. Briand,[58] G. Calderini,[58] J. Chauveau,[58] P. David,[58] L. Del Buono,[58] O. Hamon,[58] Ph. Leruste,[58] J. Ocariz,[58] A. Perez,[58] J. Prendki,[58] S. Sitt,[58] L. Gladney,[59] M. Biasini[ab],[60]

R. Covarelli[ab],[60] E. Manoni[ab],[60] C. Angelini[ab],[61] G. Batignani[ab],[61] S. Bettarini[ab],[61] M. Carpinelli[ab],[61,††] A. Cervelli[ab],[61] F. Forti[ab],[61] M. A. Giorgi[ab],[61] A. Lusiani[ac],[61] G. Marchiori[ab],[61] M. Morganti[ab],[61] N. Neri[ab],[61] E. Paoloni[ab],[61] G. Rizzo[ab],[61] J. J. Walsh[a],[61] D. Lopes Pegna,[62] C. Lu,[62] J. Olsen,[62] A. J. S. Smith,[62] A. V. Telnov,[62] F. Anulli[a],[63] E. Baracchini[ab],[63] G. Cavoto[a],[63] D. del Re[ab],[63] E. Di Marco[ab],[63] R. Faccini[ab],[63] F. Ferrarotto[a],[63] F. Ferroni[ab],[63] M. Gaspero[ab],[63] P. D. Jackson[a],[63] L. Li Gioi[a],[63] M. A. Mazzoni[a],[63] S. Morganti[a],[63] G. Piredda[a],[63] F. Polci[ab],[63] F. Renga[ab],[63] C. Voena[a],[63] M. Ebert,[64] T. Hartmann,[64] H. Schröder,[64] R. Waldi,[64] T. Adye,[65] B. Franek,[65] E. O. Olaiya,[65] F. F. Wilson,[65] S. Emery,[66] M. Escalier,[66] L. Esteve,[66] S. F. Ganzhur,[66] G. Hamel de Monchenault,[66] W. Kozanecki,[66] G. Vasseur,[66] Ch. Yèche,[66] M. Zito,[66] X. R. Chen,[67] H. Liu,[67] W. Park,[67] M. V. Purohit,[67] R. M. White,[67] J. R. Wilson,[67] M. T. Allen,[68] D. Aston,[68] R. Bartoldus,[68] P. Bechtle,[68] J. F. Benitez,[68] R. Cenci,[68] J. P. Coleman,[68] M. R. Convery,[68] J. C. Dingfelder,[68] J. Dorfan,[68] G. P. Dubois-Felsmann,[68] W. Dunwoodie,[68] R. C. Field,[68] A. M. Gabareen,[68] S. J. Gowdy,[68] M. T. Graham,[68] P. Grenier,[68] C. Hast,[68] W. R. Innes,[68] J. Kaminski,[68] M. H. Kelsey,[68] H. Kim,[68] P. Kim,[68] M. L. Kocian,[68] D. W. G. S. Leith,[68] S. Li,[68] B. Lindquist,[68] S. Luitz,[68] V. Luth,[68] H. L. Lynch,[68] D. B. MacFarlane,[68] H. Marsiske,[68] R. Messner,[68] D. R. Muller,[68] H. Neal,[68] S. Nelson,[68] C. P. O'Grady,[68] I. Ofte,[68] A. Perazzo,[68] M. Perl,[68] B. N. Ratcliff,[68] A. Roodman,[68] A. A. Salnikov,[68] R. H. Schindler,[68] J. Schwiening,[68] A. Snyder,[68] D. Su,[68] M. K. Sullivan,[68] K. Suzuki,[68] S. K. Swain,[68] J. M. Thompson,[68] J. Va'vra,[68] A. P. Wagner,[68] M. Weaver,[68] C. A. West,[68] W. J. Wisniewski,[68] M. Wittgen,[68] D. H. Wright,[68] H. W. Wulsin,[68] A. K. Yarritu,[68] K. Yi,[68] C. C. Young,[68] V. Ziegler,[68] P. R. Burchat,[69] A. J. Edwards,[69] S. A. Majewski,[69] T. S. Miyashita,[69] B. A. Petersen,[69] L. Wilden,[69] S. Ahmed,[70] M. S. Alam,[70] J. A. Ernst,[70] B. Pan,[70] M. A. Saeed,[70] S. B. Zain,[70] S. M. Spanier,[71] B. J. Wogsland,[71] R. Eckmann,[72] J. L. Ritchie,[72] A. M. Ruland,[72] C. J. Schilling,[72] R. F. Schwitters,[72] B. W. Drummond,[73] J. M. Izen,[73] X. C. Lou,[73] F. Bianchi[ab],[74] D. Gamba[ab],[74] M. Pelliccioni[ab],[74] M. Bomben[ab],[75] L. Bosisio[ab],[75] C. Cartaro[ab],[75] G. Della Ricca[ab],[75] L. Lanceri[ab],[75] L. Vitale[ab],[75] V. Azzolini,[76] N. Lopez-March,[76] F. Martinez-Vidal,[76] D. A. Milanes,[76] A. Oyanguren,[76] J. Albert,[77] Sw. Banerjee,[77] B. Bhuyan,[77] H. H. F. Choi,[77] K. Hamano,[77] R. Kowalewski,[77] M. J. Lewczuk,[77] I. M. Nugent,[77] J. M. Roney,[77] R. J. Sobie,[77] T. J. Gershon,[78] P. F. Harrison,[78] J. Ilic,[78] T. E. Latham,[78] G. B. Mohanty,[78] H. R. Band,[79] X. Chen,[79] S. Dasu,[79] K. T. Flood,[79] Y. Pan,[79] M. Pierini,[79] R. Prepost,[79] C. O. Vuosalo,[79] and S. L. Wu[79]

(The *BABAR* Collaboration)

[1] *Laboratoire de Physique des Particules, IN2P3/CNRS et Université de Savoie, F-74941 Annecy-Le-Vieux, France*
[2] *Universitat de Barcelona, Facultat de Fisica, Departament ECM, E-08028 Barcelona, Spain*
[3] *INFN Sezione di Bari[a]; Dipartmento di Fisica, Università di Bari[b], I-70126 Bari, Italy*
[4] *University of Bergen, Institute of Physics, N-5007 Bergen, Norway*
[5] *Lawrence Berkeley National Laboratory and University of California, Berkeley, California 94720, USA*
[6] *University of Birmingham, Birmingham, B15 2TT, United Kingdom*
[7] *Ruhr Universität Bochum, Institut für Experimentalphysik 1, D-44780 Bochum, Germany*
[8] *University of Bristol, Bristol BS8 1TL, United Kingdom*
[9] *University of British Columbia, Vancouver, British Columbia, Canada V6T 1Z1*
[10] *Brunel University, Uxbridge, Middlesex UB8 3PH, United Kingdom*
[11] *Budker Institute of Nuclear Physics, Novosibirsk 630090, Russia*
[12] *University of California at Irvine, Irvine, California 92697, USA*
[13] *University of California at Los Angeles, Los Angeles, California 90024, USA*
[14] *University of California at Riverside, Riverside, California 92521, USA*
[15] *University of California at San Diego, La Jolla, California 92093, USA*
[16] *University of California at Santa Barbara, Santa Barbara, California 93106, USA*
[17] *University of California at Santa Cruz, Institute for Particle Physics, Santa Cruz, California 95064, USA*
[18] *California Institute of Technology, Pasadena, California 91125, USA*
[19] *University of Cincinnati, Cincinnati, Ohio 45221, USA*
[20] *University of Colorado, Boulder, Colorado 80309, USA*
[21] *Colorado State University, Fort Collins, Colorado 80523, USA*
[22] *Technische Universität Dortmund, Fakultät Physik, D-44221 Dortmund, Germany*
[23] *Technische Universität Dresden, Institut für Kern- und Teilchenphysik, D-01062 Dresden, Germany*
[24] *Laboratoire Leprince-Ringuet, CNRS/IN2P3, Ecole Polytechnique, F-91128 Palaiseau, France*
[25] *University of Edinburgh, Edinburgh EH9 3JZ, United Kingdom*
[26] *INFN Sezione di Ferrara[a]; Dipartimento di Fisica, Università di Ferrara[b], I-44100 Ferrara, Italy*
[27] *INFN Laboratori Nazionali di Frascati, I-00044 Frascati, Italy*
[28] *INFN Sezione di Genova[a]; Dipartimento di Fisica, Università di Genova[b], I-16146 Genova, Italy*
[29] *Harvard University, Cambridge, Massachusetts 02138, USA*
[30] *Universität Heidelberg, Physikalisches Institut, Philosophenweg 12, D-69120 Heidelberg, Germany*
[31] *Humboldt-Universität zu Berlin, Institut für Physik, Newtonstr. 15, D-12489 Berlin, Germany*

[32]Imperial College London, London, SW7 2AZ, United Kingdom
[33]University of Iowa, Iowa City, Iowa 52242, USA
[34]Iowa State University, Ames, Iowa 50011-3160, USA
[35]Johns Hopkins University, Baltimore, Maryland 21218, USA
[36]Laboratoire de l'Accélérateur Linéaire, IN2P3/CNRS et Université Paris-Sud 11,
Centre Scientifique d'Orsay, B. P. 34, F-91898 Orsay Cedex, France
[37]Lawrence Livermore National Laboratory, Livermore, California 94550, USA
[38]University of Liverpool, Liverpool L69 7ZE, United Kingdom
[39]Queen Mary, University of London, London, E1 4NS, United Kingdom
[40]University of London, Royal Holloway and Bedford New College, Egham, Surrey TW20 0EX, United Kingdom
[41]University of Louisville, Louisville, Kentucky 40292, USA
[42]Johannes Gutenberg-Universität Mainz, Institut für Kernphysik, D-55099 Mainz, Germany
[43]University of Manchester, Manchester M13 9PL, United Kingdom
[44]University of Maryland, College Park, Maryland 20742, USA
[45]University of Massachusetts, Amherst, Massachusetts 01003, USA
[46]Massachusetts Institute of Technology, Laboratory for Nuclear Science, Cambridge, Massachusetts 02139, USA
[47]McGill University, Montréal, Québec, Canada H3A 2T8
[48]INFN Sezione di Milano[a]; Dipartimento di Fisica, Università di Milano[b], I-20133 Milano, Italy
[49]University of Mississippi, University, Mississippi 38677, USA
[50]Université de Montréal, Physique des Particules, Montréal, Québec, Canada H3C 3J7
[51]Mount Holyoke College, South Hadley, Massachusetts 01075, USA
[52]INFN Sezione di Napoli[a]; Dipartimento di Scienze Fisiche,
Università di Napoli Federico II[b], I-80126 Napoli, Italy
[53]NIKHEF, National Institute for Nuclear Physics and High Energy Physics, NL-1009 DB Amsterdam, The Netherlands
[54]University of Notre Dame, Notre Dame, Indiana 46556, USA
[55]Ohio State University, Columbus, Ohio 43210, USA
[56]University of Oregon, Eugene, Oregon 97403, USA
[57]INFN Sezione di Padova[a]; Dipartimento di Fisica, Università di Padova[b], I-35131 Padova, Italy
[58]Laboratoire de Physique Nucléaire et de Hautes Energies,
IN2P3/CNRS, Université Pierre et Marie Curie-Paris6,
Université Denis Diderot-Paris7, F-75252 Paris, France
[59]University of Pennsylvania, Philadelphia, Pennsylvania 19104, USA
[60]INFN Sezione di Perugia[a]; Dipartimento di Fisica, Università di Perugia[b], I-06100 Perugia, Italy
[61]INFN Sezione di Pisa[a]; Dipartimento di Fisica,
Università di Pisa[b]; Scuola Normale Superiore di Pisa[c], I-56127 Pisa, Italy
[62]Princeton University, Princeton, New Jersey 08544, USA
[63]INFN Sezione di Roma[a]; Dipartimento di Fisica,
Università di Roma La Sapienza[b], I-00185 Roma, Italy
[64]Universität Rostock, D-18051 Rostock, Germany
[65]Rutherford Appleton Laboratory, Chilton, Didcot, Oxon, OX11 0QX, United Kingdom
[66]CEA, Irfu, SPP, Centre de Saclay, F-91191 Gif-sur-Yvette, France
[67]University of South Carolina, Columbia, South Carolina 29208, USA
[68]Stanford Linear Accelerator Center, Stanford, California 94309, USA
[69]Stanford University, Stanford, California 94305-4060, USA
[70]State University of New York, Albany, New York 12222, USA
[71]University of Tennessee, Knoxville, Tennessee 37996, USA
[72]University of Texas at Austin, Austin, Texas 78712, USA
[73]University of Texas at Dallas, Richardson, Texas 75083, USA
[74]INFN Sezione di Torino[a]; Dipartimento di Fisica Sperimentale, Università di Torino[b], I-10125 Torino, Italy
[75]INFN Sezione di Trieste[a]; Dipartimento di Fisica, Università di Trieste[b], I-34127 Trieste, Italy
[76]IFIC, Universitat de Valencia-CSIC, E-46071 Valencia, Spain
[77]University of Victoria, Victoria, British Columbia, Canada V8W 3P6
[78]Department of Physics, University of Warwick, Coventry CV4 7AL, United Kingdom
[79]University of Wisconsin, Madison, Wisconsin 53706, USA

(Dated: November 14, 2008)

We report a search for the decays $B^- \to K^+\pi^-\pi^-$ and $B^- \to K^-K^-\pi^+$, which are highly suppressed in the standard model. Using a sample of $(467 \pm 5) \times 10^6$ $B\overline{B}$ pairs collected with the *BABAR* detector, we do not see any evidence of these decays and determine 90% confidence level upper limits of $\mathcal{B}(B^- \to K^+\pi^-\pi^-) < 9.5 \times 10^{-7}$ and $\mathcal{B}(B^- \to K^-K^-\pi^+) < 1.6 \times 10^{-7}$ on the corresponding branching fractions, including systematic uncertainties.

PACS numbers: 13.25.Hw, 12.60.-i

The decays $B^- \to K^+\pi^-\pi^-$ and $B^- \to K^-K^-\pi^+$ proceed via $b \to dd\overline{s}$ and $b \to ss\overline{d}$ quark transitions, respectively. These are highly suppressed in the standard model (SM). Compared with the penguin (loop) transitions $b \to q\overline{q}d$, and $b \to q\overline{q}s$ they are additionally suppressed by the small Cabibbo-Kobayashi-Maskawa matrix [1, 2] element factor $|V_{td}V_{ts}^*| \simeq 3 \times 10^{-4}$, leading to predicted branching fractions of only $\mathcal{O}(10^{-14})$ and $\mathcal{O}(10^{-11})$, respectively [3, 4]. Example SM decay diagrams can be seen in Fig. 1.

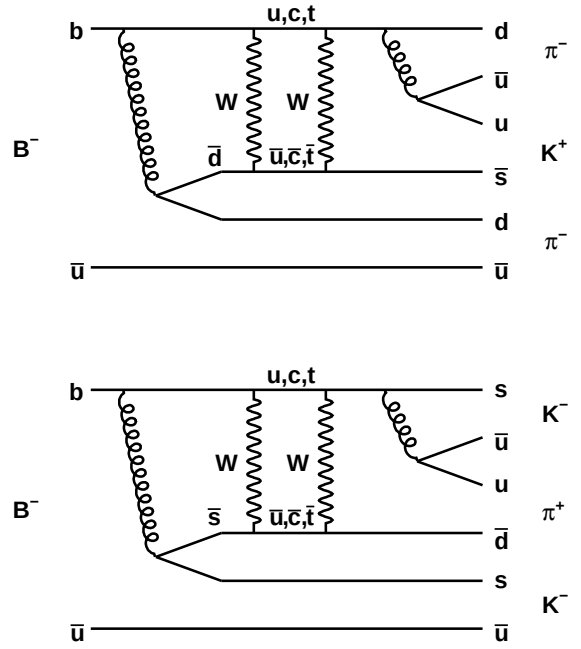

FIG. 1: Example standard model decay diagrams for the decays $B^- \to K^+\pi^-\pi^-$ and $B^- \to K^-K^-\pi^+$, respectively.

These branching fractions can be significantly enhanced in SM extensions such as the minimal supersymmetric standard model (MSSM) with or without conserved R parity, or in models containing extra $U(1)$ gauge bosons. For example, the branching fraction for the $b \to dd\overline{s}$ transition $B^- \to \pi^- K^{*0}$ can be enhanced from about 10^{-16} in the SM to about 10^{-6} in the presence of an extra Z' boson [4]. The branching fraction for the $b \to ss\overline{d}$ decay $B^- \to K^-\overline{K}^{*0}$ can be enhanced from about 7×10^{-14} in the SM to about 6×10^{-9} in the MSSM [5].

Observations of the decays $B^- \to K^+\pi^-\pi^-$ and $B^- \to K^-K^-\pi^+$ would be clear experimental signals for the $b \to dd\overline{s}$ and $b \to ss\overline{d}$ quark transitions [6, 7]. These decay modes have been previously searched for [8, 9, 10, 11], and the most restrictive 90% confidence level experimental upper limits $\mathcal{B}(B^- \to K^+\pi^-\pi^-) < 1.8 \times 10^{-6}$ and $\mathcal{B}(B^- \to K^-K^-\pi^+) < 1.3 \times 10^{-6}$ [10] were obtained from an analysis of 81.8 fb^{-1} of *BABAR* data. Upper limits on $b \to ss\overline{d}$ transitions have also been set using the decays $B^- \to K^{*-}K^-\pi^+$ [12], $\overline{B}^0 \to \overline{K}^{*0}K^-\pi^+$ [13], and $\overline{B}^0 \to \overline{K}^{*0}\overline{K}^{*0}$ [14].

We report the results of a search for the decays $B^- \to K^+\pi^-\pi^-$ and $B^- \to K^-K^-\pi^+$. Inclusion of the charge conjugate modes is implied throughout this paper. The data used in this analysis, collected at the PEP-II asymmetric energy e^+e^- collider [15], consist of an integrated luminosity of 426 fb^{-1} recorded at the $\Upsilon(4S)$ resonance. In addition, 44 fb^{-1} of data were collected 40 MeV below the resonance and are used for background characterization. These samples are referred to as on-resonance and off-resonance data, respectively. The on-resonance data sample contains $(467 \pm 5) \times 10^6$ $B\overline{B}$ pairs. Beyond the larger sample size, we utilize improved analysis techniques for background rejection and signal identification compared with our previous study [10].

The *BABAR* detector is described in detail elsewhere [16]. Charged particles are detected and their momenta measured with a five-layer silicon vertex tracker and a 40-layer drift chamber (DCH) inside a 1.5 T solenoidal magnet. Surrounding the DCH is a detector of internally reflected Cherenkov radiation. Energy deposited by electrons and photons is measured by a CsI(Tl) crystal electromagnetic calorimeter.

We select $B^- \to K^+\pi^-\pi^-$ candidates by combining a charged kaon candidate with two charged pion candidates, each of which has charge opposite to the kaon. Similarly, $B^- \to K^-K^-\pi^+$ candidates are selected by combining two charged kaon candidates with a charged pion candidate. Each track is required to have a minimum transverse momentum of 50 MeV/c, and to be consistent with having originated from the interaction region. Identification of charged pions and kaons is accomplished using energy loss ($\mathrm{d}E/\mathrm{d}x$) information from the silicon vertex tracker and DCH, and the Cherenkov angle and number of photons measured in the detector of internally reflected Cherenkov radiation. The efficiency for kaon selection is approximately 80% including geometrical acceptance, while the probability of misidentification of pions as kaons is below 5%. The corresponding efficiency and kaon misindentification rate for the pion selection criteria are 95% and less than 10%, respectively. We require all charged particle candidates to be inconsistent with the electron hypothesis, based on a cut-based selection algorithm that uses information from $\mathrm{d}E/\mathrm{d}x$, shower shapes in the electromagnetic calorimeter, and the ratio

*Deceased
†Now at Temple University, Philadelphia, Pennsylvania 19122, USA
‡Now at Tel Aviv University, Tel Aviv, 69978, Israel
§Also with Università di Perugia, Dipartimento di Fisica, Perugia, Italy
¶Also with Università di Roma La Sapienza, I-00185 Roma, Italy
**Now at University of South Alabama, Mobile, Alabama 36688, USA
††Also with Università di Sassari, Sassari, Italy

of the shower energy and track momentum.

To avoid a potentially large source of background arising from B decays mediated by the favored $b \to c$ transition, we veto B candidates for which pairs of daughter tracks have invariant mass combinations in the ranges $1.76 < m_{K\pi} < 1.94\,\mathrm{GeV}/c^2$, $2.85 < m_{K\pi} < 3.25\,\mathrm{GeV}/c^2$, and $3.65 < m_{K\pi} < 3.75\,\mathrm{GeV}/c^2$. These remove events containing the decays $D^0 \to K^-\pi^+$, $J/\psi \to \ell^+\ell^-$, and $\psi(2S) \to \ell^+\ell^-$, respectively, where the leptons in the J/ψ and $\psi(2S)$ decays are misidentified as pions or kaons.

Continuum $e^+e^- \to q\overline{q}$ ($q = u, d, s, \rangle$ events are the dominant background. To discriminate this type of event from signal, we use a neural network that combines five variables. The first of these is the ratio of L_2 to L_0, with $L_j = \sum_i p_i^\star\,|\cos\theta_i^\star|^j$, where $p_i^\star$ is the particle momentum, $\theta_i^\star$ is the angle between the particle and the thrust axis determined from the B candidate decay products, the sum is over all tracks and neutral clusters not associated with the B candidate, and all quantities are calculated in the e^+e^- center-of-mass (CM) frame. The other four variables are the absolute value of the cosine of the angle between the B direction and the beam axis; the magnitude of the cosine of the angle between the B thrust axis and the beam axis; the product of the B candidate's charge and the output of a multivariate algorithm that identifies the flavor of the recoiling B meson [17]; and the proper time difference between the decays of the two B mesons divided by its uncertainty. The angles with respect to the beam axis are calculated in the CM frame. The neural network output $\mathrm{NN_{out}}$ is distributed such that it peaks around 0 for continuum background and around 1 for signal. We require $\mathrm{NN_{out}} > 0.5$ ($\mathrm{NN_{out}} > 0.4$) for $B^- \to K^+\pi^-\pi^-$ ($B^- \to K^-K^-\pi^+$) candidates. These requirements retain approximately 90% of the signal, while rejecting approximately 80% of the continuum background.

In addition to the neural network output, we distinguish signal from background events using two kinematic variables: the difference ΔE between the CM energy of the B candidate and $\sqrt{s}/2$, and the beam-energy substituted mass $m_{\mathrm{ES}} = \sqrt{s/4 - \mathbf{p}_B^{\star 2}}$, where $\sqrt{s}$ is the total CM energy and $\mathbf{p}_B^\star$ is the momentum of the candidate B meson in the CM frame. The ΔE distribution peaks near zero with a resolution of around 19 MeV, while the m_{ES} distribution for signal events peaks near the B mass with a resolution of around $2.4\,\mathrm{MeV}/c^2$. We select signal candidates that satisfy $5.260 < m_{\mathrm{ES}} < 5.286\,\mathrm{GeV}/c^2$ and $|\Delta E| < 0.100\,\mathrm{GeV}$. This region includes a sufficiently large range of m_{ES} below the signal peak to determine properties of the continuum distribution.

The efficiency for signal events to pass the selection criteria is 21.6% (17.8%) for $B^- \to K^+\pi^-\pi^-$ ($B^- \to K^-K^-\pi^+$), determined with a Monte Carlo (MC) simulation in which the decays are generated uniformly in three-body phase space. The *BABAR* detector Monte Carlo simulation is based on `GEANT` 4 [18] and `EvtGen` [19]. We find that 8.2% (5.1%) of $B^- \to K^+\pi^-\pi^-$ ($B^- \to K^-K^-\pi^+$) selected events contain more than one candidate, in which case we choose the one with the highest probability that the three tracks originate from a common vertex.

We study possible residual backgrounds from $B\overline{B}$ events using MC event samples. Backgrounds arise from decays with topologies similar to the signal but with some misreconstruction. Such effects include kaon/pion misidentification, the loss of a soft neutral particle, and the association of a particle from the decay of the other B in the event with the signal candidate or vice versa. We find that the backgrounds can be conveniently divided into five categories for both the $K^+\pi^-\pi^-$ and $K^-K^-\pi^+$ channels, each of which is dominated by one or two particular decays but also includes other decay modes that result in similar m_{ES} and ΔE shapes. Table I provides details of the composition of the background categories.

In order to obtain the $B^- \to K^+\pi^-\pi^-$ and $B^- \to K^-K^-\pi^+$ signal yields, we perform unbinned extended maximum likelihood fits to the candidate events using three variables: m_{ES}, ΔE, and $\mathrm{NN_{out}}$. For each event hypothesis j (signal, continuum background, or one of the five $B\overline{B}$ background categories), we define a probability density function (PDF)

$$\mathcal{P}_j^i \equiv \mathcal{P}_j({m_{\mathrm{ES}}}^i, \Delta E^i) \cdot \mathcal{P}_j(\mathrm{NN}_{\mathrm{out}}^i)\,, \qquad (1)$$

where i denotes the event index. For the signal, continuum background, and the $B\overline{B}$ background categories with small correlations between m_{ES} and ΔE, the PDF is further factorized

$$\mathcal{P}_j({m_{\mathrm{ES}}}^i, \Delta E^i) = \mathcal{P}_j({m_{\mathrm{ES}}}^i) \cdot \mathcal{P}_j(\Delta E^i)\,. \qquad (2)$$

The extended likelihood function is

$$\mathcal{L} = \exp\left(-\sum_k n_k\right) \prod_i \left[\sum_j n_j \mathcal{P}_j^i\right], \qquad (3)$$

where n_j (n_k) is the yield belonging to the event hypothesis j (k).

The signal m_{ES} and ΔE shapes are parametrized with the sum of a Gaussian and a Crystal Ball function [20, 21, 22] and the sum of two Gaussian functions, respectively. We determine the shape parameters by taking the values obtained from signal MC and correcting for differences between data and MC seen in a control sample of $B^- \to D^0\pi^-$ with $D^0 \to K^-\pi^+$ decays. The continuum background m_{ES} shape is described by the function $x\sqrt{1-x^2}\exp\left[-\xi(1-x^2)\right]$, with $x \equiv 2m_{\mathrm{ES}}/\sqrt{s}$ and ξ a free parameter [23], while the continuum ΔE shape is modeled with a linear function. We describe the m_{ES} and ΔE shapes of each $B\overline{B}$ background category using either independent 1D histograms or a 2D histogram determined from MC samples. The decision to use 1D or 2D histograms is made based on the magnitude of the correlations between these variables for each category and the effect on the signal yield of neglecting such correlations, discussed below. The PDFs for categories 1, 2, and 3, for both $B^- \to K^+\pi^-\pi^-$ and $B^- \to K^-K^-\pi^+$,

TABLE I: Summary of the B background categories, giving the dominant decay mode, numbers of expected and observed events and the character of the $m_{\rm ES}$ and ΔE distributions. "Peaking" indicates that the shape is similar to that of the signal. "Broad peak," "left peak," and "right peak" differ from the signal in being wider or shifted to lower or higher values, respectively. The number of expected and observed events are also given for the continuum background.

$B^- \to K^+\pi^-\pi^-$						
Category	1	2	3	4	5	Continuum
Dominant mode(s)	$B^- \to D^0\pi^-$; $D^0 \to K^-K^+$	$B^- \to \pi^-\pi^+\pi^-$	$B^- \to K^-\pi^+\pi^-$& $B^0 \to K^+\pi^-\pi^0$	$B^0 \to K^+\pi^-$	Generic $B\overline{B}$	$\cdots$
Number of expected events	80 ± 3	57 ± 4	472 ± 24	43 ± 1	917 ± 19	25552 ± 495
Number of observed events	61 ± 70	-153 ± 94	1116 ± 347	-26 ± 152	197 ± 273	25261 ± 198
$m_{\rm ES}$ Structure	Peaking	Peaking	Broad peak	Broad peak	Continuum-like	$\cdots$
ΔE Structure	Left peak	Right peak	Broad peak	Right peak	Continuum-like	$\cdots$
$B^- \to K^-K^-\pi^+$						
Category	1	2	3	4	5	Continuum
Dominant mode(s)	$B^- \to K^-K^+K^-$	$B^- \to K^-\pi^+\pi^-$	$B^- \to D^0\pi^-$; $D^0 \to K^-\pi^+\pi^0$	Generic B^+B^-	Generic $B^0\overline{B}^0$	$\cdots$
Number of expected events	190 ± 9	198 ± 9	61 ± 4	312 ± 11	173 ± 8	6088 ± 241
Number of observed events	213 ± 41	240 ± 37	-34 ± 55	380 ± 117	95 ± 107	6953 ± 100
$m_{\rm ES}$ Structure	Peaking	Peaking	Broad peak	Broad peak	Continuum-like	$\cdots$
ΔE Structure	Left peak	Right peak	Left peak	Continuum-like	Continuum-like	$\cdots$

are modeled using 2D histograms. We use 1D histograms to describe all $\rm NN_{out}$ distributions. These histograms are obtained from MC samples for the signal and $B\overline{B}$ background categories, and from a combination of on-resonance data, in a continuum-dominated sideband of $m_{\rm ES}$ and ΔE, and off-resonance data for the continuum background.

The nine free parameters in our fits are the yields of the signal, continuum and all five $B\overline{B}$ background categories, the ξ parameter of the continuum $m_{\rm ES}$ shape, and the slope of the continuum ΔE shape.

We test the fitting procedure by applying it to ensembles of simulated experiments where events are generated from the PDF shapes described above for all seven categories of events. We repeat the exercise with $q\overline{q}$ events generated from the PDF while signal events are randomly extracted from the MC samples. The $B\overline{B}$ background events are either generated from PDF shapes or drawn from MC samples. In all cases, these tests confirm that our fit performs as expected, with very small biases on the fitted signal yields, for which we correct the measured yields and include systematic uncertainties.

We apply the fit described above to the 26 478 $B^- \to K^+\pi^-\pi^-$ and 7 822 $B^- \to K^-K^-\pi^+$ candidate events selected from the data recorded at the $\Upsilon(4S)$ resonance. We find 22 ± 43 and -26 ± 19 signal events, respectively, (statistical uncertainties only). The yields of continuum and all $B\overline{B}$ background categories (shown in Table I) are generally consistent with expectations. The yields of $B\overline{B}$ background categories 3 and 5 from the fit to $B^- \to K^+\pi^-\pi^-$ candidates do not show perfect agreement; however, the sum of their yields is consistent with the expectation and, owing to the strong negative correlation between the yields of these categories, the discrepancy with the expectation is not significant. Such behavior was seen in the fit validations and has been shown not to effect the signal yield. The results of the fits are shown in Fig. 2.

We determine the branching fractions for $B^- \to K^+\pi^-\pi^-$ and $B^- \to K^-K^-\pi^+$ by applying corrections for the small biases evaluated in the MC studies (3.6 ± 2.4 and 0.5 ± 1.0 events, respectively) and then dividing by the selection efficiencies and the total number of $B\overline{B}$ pairs in the data sample. We assume equal decay rates of $\Upsilon(4S) \to B^+B^-$ and $B^0\overline{B}^0$. Systematic uncertainties on the fitted yields arise from uncertainties in the PDF shapes (10.0 and 3.5 events, respectively) including possible data/MC differences in the signal PDF shapes studied using the $B^- \to D^0\pi^-$ control samples discussed above. We estimate the uncertainty on the fit bias (3.1 and 1.0 events, respectively) to be half the value of the correction combined in quadrature with the precision with which the bias is known. Uncertainties on the efficiency arise from possible data/MC differences for tracking (1.2%) and particle identification (4.2%). We consider two sources of uncertainty related to the Dalitz plot distributions of the signal decays. The first is related to the variation of the efficiency over the parts of the Dalitz plots that are included in the analysis: from MC studies, the uncertainties are found to be 13.0% for $B^- \to K^+\pi^-\pi^-$ and 13.5% for $B^- \to K^-K^-\pi^+$. The second is due to the correction for the vetoed parts of the Dalitz plots, which we estimate for various signal decay distributions. In addition to the nominal phase-space distribution, we consider decays dominated by the intermediate states $K^{*0}(892)$ or $K_0^{*0}(1430)$ (modeled using the LASS [24] shape, as implemented in our Dalitz plot analysis of $B^+ \to K^+\pi^-\pi^+$ [25]). We mimic a possible enhancement at low $\pi^-\pi^-$ or

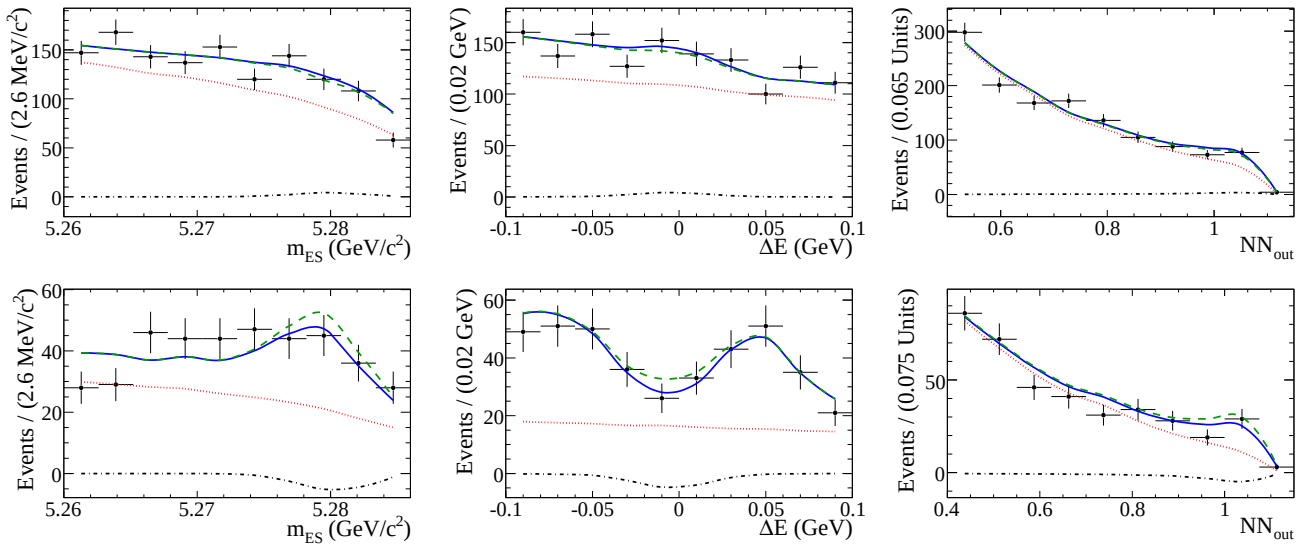

FIG. 2: Projections of the selected events with the fit results overlaid. The top (bottom) set of plots are for $B^- \to K^+\pi^-\pi^-$ ($B^- \to K^-K^-\pi^+$). From left to right the plots show the projections onto $m_{\rm ES}$, ΔE, and the output of the neural network. The black points are the data, the solid blue curve is the total fit, the dotted red curve is the continuum background, the dashed green curve is the total background, and the dash-dotted black curve at the bottom is the signal. The continuum component has been suppressed in these plots by applying an additional requirement on the ratio of the signal likelihood to the sum of the signal and continuum likelihoods, calculated without use of the plotted variable. The value of the requirement for each plot is chosen to reject about 95% of the continuum background while retaining about 55% of the signal.

K^-K^- invariant mass by employing an *ad hoc* doubly charged scalar resonance with mass 1500 MeV/c^2 and width 300 MeV/c^2. The efficiency of the veto requirement is larger than that for the phase-space MC in all alternative models, so we assign asymmetric systematic errors of $^{+0\%}_{-18\%}$ for $B^- \to K^+\pi^-\pi^-$ and $^{+25\%}_{-0\%}$ for $B^- \to K^-K^-\pi^+$. The uncertainty on the number of $B\overline{B}$ pairs is 1.1%. Including all systematic uncertainties, we obtain the following results for the branching fractions: $\mathcal{B}(B^- \to K^+\pi^-\pi^-) = (1.8 \pm 4.3 \pm 0.9) \times 10^{-7}$ and $\mathcal{B}(B^- \to K^-K^-\pi^+) = (-3.2 \pm 2.3\,^{+1.0}_{-0.6}) \times 10^{-7}$, where the first uncertainties are statistical and the second are systematic.

We have also calculated the branching fractions using event-by-event efficiencies applied to signal weights obtained from the fit result [26, 27]. We obtain results consistent with our main results within the efficiency variation systematic uncertainty. We have also checked that removing each of the discriminating variables from the fit, in turn, gives consistent results.

To obtain 90% confidence level upper limits on the branching fractions, we use the frequentist approach of Feldman and Cousins [28]. We determine 90% confidence region bands that relate the true values of the branching fractions to the measured numbers of signal events. These bands are constructed using the results of MC studies that account for relevant biases in the fit procedure and include systematic uncertainties. The construction of the confidence region bands is shown in Fig. 3. The 90% confidence level upper limits are found to be $\mathcal{B}(B^- \to K^+\pi^-\pi^-) < 9.5 \times 10^{-7}$ and $\mathcal{B}(B^- \to K^-K^-\pi^+) < 1.6 \times 10^{-7}$. To aid comparison with other experiments, we also extract the sensitivities $\mathcal{B}_0$ defined as the 90% confidence level upper limits that would be obtained in the case of zero fitted signal yield. The sensitivities are $\mathcal{B}_0(B^- \to K^+\pi^-\pi^-) < 7.4 \times 10^{-7}$ and $\mathcal{B}_0(B^- \to K^-K^-\pi^+) < 4.2 \times 10^{-7}$.

In conclusion, we present searches for the standard model suppressed B meson decays $B^- \to K^+\pi^-\pi^-$ and $B^- \to K^-K^-\pi^+$. We do not see any evidence of these decays and obtain improved 90% confidence level upper limits on the branching fractions. These results supersede those of our previous publication [10] and can be used to constrain models of new physics.

We are grateful for the excellent luminosity and machine conditions provided by our PEP-II colleagues, and for the substantial dedicated effort from the computing organizations that support *BABAR*. The collaborating institutions wish to thank SLAC for its support and kind hospitality. This work is supported by DOE and NSF (USA), NSERC (Canada), CEA and CNRS-IN2P3 (France), BMBF and DFG (Germany), INFN (Italy), FOM (The Netherlands), NFR (Norway), MES (Russia), MEC (Spain), and STFC (United Kingdom). Individuals have received support from the Marie Curie EIF (European Union) and the A. P. Sloan Foundation.

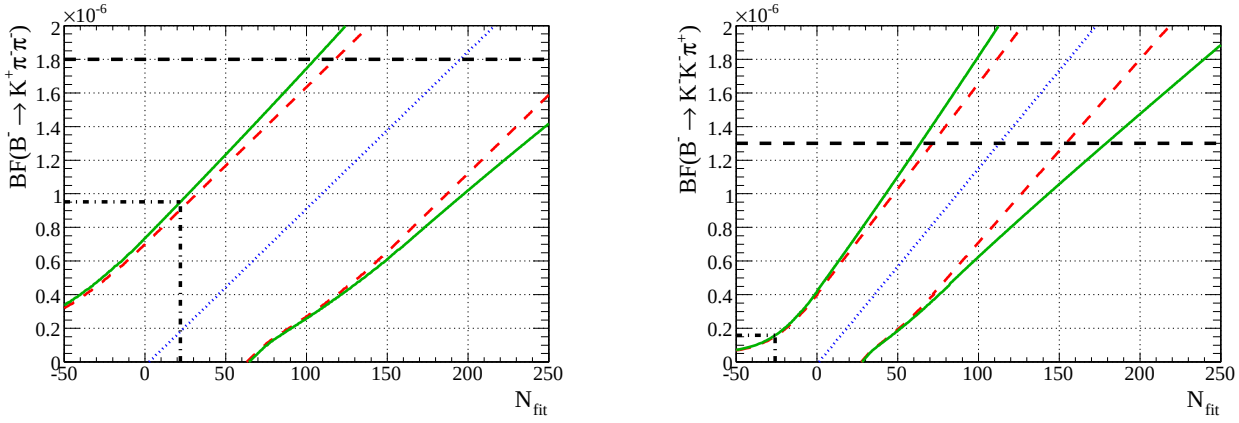

FIG. 3: Construction of the confidence region bands. The left (right) plot is for $B^- \to K^+\pi^-\pi^-$ ($B^- \to K^-K^-\pi^+$). In each figure the blue dotted line shows the expected central value of $N_{\rm fit}$ as a function of the true branching fraction, the green solid (red dashed) lines show the 90% confidence level upper and lower limits including statistical and systematic errors (statistical errors only), the black dashed horizontal line marks the position of the previous upper limit [10], and the black dash-dotted lines indicate the results of this study.

[1] N. Cabibbo, Phys. Rev. Lett. **10**, 531 (1963).
[2] M. Kobayashi and T. Maskawa, Prog. Theor. Phys. **49**, 652 (1973).
[3] K. Huitu, D. X. Zhang, C. D. Lu, and P. Singer, Phys. Rev. Lett. **81**, 4313 (1998).
[4] S. Fajfer, J. F. Kamenik, and N. Kosnik, Phys. Rev. **D74**, 034027 (2006).
[5] S. Fajfer and P. Singer, Phys. Rev. **D62**, 117702 (2000).
[6] E. J. Chun and J. S. Lee (2003), hep-ph/0307108.
[7] T. E. Browder, T. Gershon, D. Pirjol, A. Soni, and J. Zupan (2008), arXiv:0802.3201 [hep-ph].
[8] T. Bergfeld et al. (CLEO Collaboration), Phys. Rev. Lett. **77**, 4503 (1996).
[9] G. Abbiendi et al. (OPAL Collaboration), Phys. Lett. **B476**, 233 (2000).
[10] B. Aubert et al. (*BABAR* Collaboration), Phys. Rev. Lett. **91**, 051801 (2003).
[11] A. Garmash et al. (Belle Collaboration), Phys. Rev. **D69**, 012001 (2004).
[12] B. Aubert et al. (*BABAR* Collaboration), Phys. Rev. **D74**, 051104 (2006).
[13] B. Aubert et al. (*BABAR* Collaboration), Phys. Rev. **D76**, 071104 (2007).
[14] B. Aubert et al. (*BABAR* Collaboration), Phys. Rev. Lett. **100**, 081801 (2008).
[15] W. Kozanecki, Nucl. Instrum. Methods Phys. Res., Sect. A **446**, 59 (2000).
[16] B. Aubert et al. (*BABAR* Collaboration), Nucl. Instrum. Methods Phys. Res., Sect. A **479**, 1 (2002).
[17] B. Aubert et al. (*BABAR* Collaboration), Phys. Rev. Lett. **94**, 161803 (2005).
[18] S. Agostinelli et al. (GEANT4 Collaboration), Nucl. Instrum. Methods Phys. Res., Sect. A **506**, 250 (2003).
[19] D. J. Lange, Nucl. Instrum. Methods Phys. Res., Sect. A **462**, 152 (2001).
[20] M. Oreglia (1980), PhD Thesis, SLAC-0236, Appendix D.
[21] J. Gaiser (1982), PhD Thesis, SLAC-0255, Appendix F.
[22] T. Skwarnicki (1986), PhD Thesis, DESY-F31-86-02, Appendix E.
[23] H. Albrecht et al. (ARGUS Collaboration), Z. Phys. **C48**, 543 (1990).
[24] D. Aston et al., Nucl. Phys. **B296**, 493 (1988).
[25] B. Aubert et al. (*BABAR* Collaboration), Phys. Rev. **D78**, 012004 (2008).
[26] M. Pivk and F. R. Le Diberder, Nucl. Instrum. Methods Phys. Res., Sect. A **555**, 356 (2005).
[27] B. Aubert et al. (*BABAR* Collaboration), Phys. Rev. Lett. **99**, 221801 (2007).
[28] G. J. Feldman and R. D. Cousins, Phys. Rev. **D57**, 3873 (1998).